LHCb Note 2006-047, PHYS
LPHE Note 2006-015
August 25, 2006

Sensitivity to the B_s–$\overline{B}_s$ Mixing Phase at LHCb[†]

Luis Fernández

LPHE, Ecole Polytechnique Fédérale de Lausanne, Switzerland

On behalf of the LHCb collaboration

We present the sensitivity to the B_s–$\overline{B}_s$ mixing phase ϕ_s at LHCb, using decays proceeding through $\bar{b} \to \bar{c}c\bar{s}$ quark-level transitions. The performance is assessed by means of toy Monte Carlo simulations, parameterized using the results of full Monte Carlo studies. Both the $\bar{b} \to \bar{c}c\bar{s}$ decays to pure ($B_s \to \eta_c\phi$, $B_s \to D_sD_s$, $B_s \to J/\psi\eta$) and to an admixture of CP eigenstates ($B_s \to J/\psi\phi$) are considered, and used to probe the B_s–$\overline{B}_s$ mixing phase through a time-dependent mixing-induced CP measurement.

PACS numbers: 11.30.Er, 12.15.Ff, 12.15.Hh, 13.25.Hw, 14.40.Nd

[†] "Physics at LHC" conference proceedings, 3–8 July 2006, Cracow, Poland.

1. Neutral B_s–$\overline{B}_s$ System

The description of CP violation in the Standard Model (SM) is based on the CKM picture [1, 2]. The unitary CKM matrix connects the electroweak eigenstates (d', s', b') of the down-type quarks with their mass eigenstates (d, s, b). The complex couplings in the CKM matrix allow CP violation to occur in the quark sector of the SM, provided we have complex physical phases, and at least three generations of quarks.

The unitarity of the quark mixing matrix leads to orthogonality relations that can be represented as triangles in the complex plane. For the B_s–$\overline{B}_s$ system, the relevant orthogonality relation is:

$$\underbrace{V_{us}V_{ub}^*}_{\mathcal{O}(\lambda^4)} + \underbrace{V_{cs}V_{cb}^*}_{\mathcal{O}(\lambda^2)} + \underbrace{V_{ts}V_{tb}^*}_{\mathcal{O}(\lambda^2)} = 0 \ , \tag{1}$$

where relative sizes are indicated using Wolfenstein's parameterization [3]. The corresponding triangle is squashed. The relevant rephasing invariant angle for the study of CP violation is doubly Cabibbo-suppressed:

$$\beta_s \equiv \chi \equiv \arg\left[-\frac{V_{cb}V_{cs}^*}{V_{tb}V_{ts}^*}\right] \approx \lambda^2\eta + \mathcal{O}(\lambda^4) \approx \arg(V_{ts}) - \pi \ . \tag{2}$$

1.1. Mixing

The neutral B_s–$\overline{B}_s$ system exhibits particle-antiparticle mixing [4]. In the following, we adopt the phase and sign conventions of [5]. The B_s–$\overline{B}_s$ mixing refers to the transitions between the two flavor eigenstates, which are not weak eigenstates, caused by the off-diagonal terms in the effective Hamiltonian describing the particle-antiparticle system. The physical mass eigenstates are defined by $|B_{L,H}\rangle = p\,|B_s\rangle \pm q\,|\overline{B}_s\rangle$.

The physical states propagate with well-defined and measurable masses ($M_{H/L}$) and decay widths ($\Gamma_{H/L}$). Their mass difference is $\Delta M_s = M_H - M_L > 0$, and their total width difference is $\Delta\Gamma_s = \Gamma_L - \Gamma_H$. The SM predictions for the mixing observables are a non-negligible $\Delta\Gamma_s/\Gamma_s \sim 10^{-1}$ (with $\Gamma_s = (\Gamma_H + \Gamma_L)/2$), and a fast oscillation frequency $\Delta M_s \sim 20\,\mathrm{ps}^{-1}$.

The particle-antiparticle transitions ($|\Delta F| = 2$) arise within the SM from box diagrams as shown in Fig. 1. The off-diagonal elements of the mass matrix, M_{12}, are dominated by internal top-quark exchanges. Since the intermediate states appearing in the determination of M_{12} are virtual, New Physics (NP) could easily contribute to it. On the other hand, the off-diagonal elements of the decay matrix, Γ_{12}, are dominated by real states to which both B_s and $\overline{B}_s$ may decay. Thus, Γ_{12} is almost insensitive to NP.

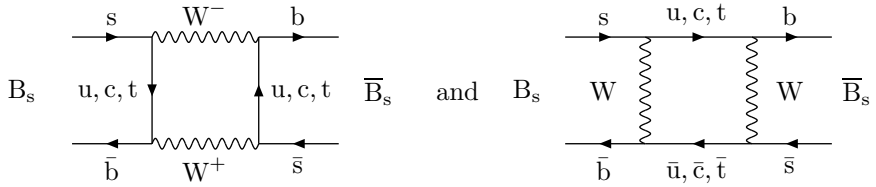

Fig. 1. Leading order box diagrams contributing to the B_s–$\overline{B}_s$ mixing in the SM.

The phase difference between M_{12} and Γ_{12} represents an observable CP-violating phase. In the SM, it reduces to the B_s–$\overline{B}_s$ mixing phase:

$$\phi_s^{SM} = 2\arg[V_{ts}^* V_{tb}] \approx -2\beta_s \sim \mathcal{O}(-0.04)\ \mathrm{rad}\ . \tag{3}$$

The SM value of ϕ_s is very small. Thus, any significant deviation from the SM expectations ($\phi_s = \phi_s^{SM} + \phi_s^{NP}$) would uncover NP.

1.2. $\bar{b} \to \bar{c}c\bar{s}$ Quark-Level Transitions

The study of B_s decays to CP eigenstates proceeding through $\bar{b} \to \bar{c}c\bar{s}$ quark-level transitions enables the determination of the B_s–$\overline{B}_s$ mixing phase ϕ_s. These decays are dominated by the tree-diagram phase, and receive negligible – doubly Cabibbo-suppressed – contributions from penguin diagrams.

There are several decays of interest for the determination of ϕ_s:

- CP-even eigenstates ($\eta_f = +1$): $\mathrm{B_s} \to \eta_c\phi$, $\mathrm{B_s} \to \mathrm{D_s D_s}$, $\mathrm{B_s} \to \mathrm{J}/\psi\eta^{(\prime)}$.
- Admixture of CP eigenstates: $\mathrm{B_s} \to \mathrm{J}/\psi\phi$. The separation of the different states is required, with CP eigenvalues $\eta_f = +1, -1, +1$. The corresponding components will be denoted by $0, \perp, \parallel$, respectively.

$\mathrm{B_s} \to \mathrm{D_s D_s}$ being color-allowed, it may be affected by final state interactions.

The phase mismatch between the mixing and decay phases allows us to perform a time-dependent mixing-induced CP measurement (see Fig. 2). The relevant complex observable for the description of CP violation in $\bar{\mathrm{b}} \to \bar{\mathrm{c}}\mathrm{c}\bar{\mathrm{s}}$ quark-level transitions is:

$$\lambda_f \equiv \frac{q}{p}\frac{\overline{A}_f}{A_f} \approx \eta_f e^{-i\phi_\mathrm{s}}\,, \qquad (4)$$

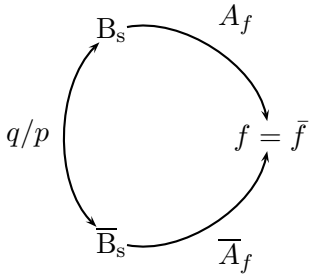

Fig. 2. Mixing-induced CP violation.

where we ignored CP violation in the mixing (i.e. $q/p = -e^{-i\phi_\mathrm{s}}$). We assume the decay amplitudes to be controlled by a single weak phase $\phi_\mathrm{D} \equiv \arg[V_\mathrm{cb}V_\mathrm{cs}^*] = \mathcal{O}(\lambda^6)$, which is approximatively real (such that the ratio of decay amplitudes is $\overline{A}_f/A_f = -\eta_f e^{i2\phi_\mathrm{D}} \approx -\eta_f$).

The decay rates for initially pure $\mathrm{B_s}$ or $\overline{\mathrm{B}}_\mathrm{s}$ states in $\bar{\mathrm{b}} \to \bar{\mathrm{c}}\mathrm{c}\bar{\mathrm{s}}$ or $\mathrm{b} \to \mathrm{c}\bar{\mathrm{c}}\mathrm{s}$ quark-level transitions are given by the following expressions for the CP components:

$$R_f\,(t,q) \;\propto\; e^{-\Gamma_\mathrm{s} t}\left\{\cosh\frac{\Delta\Gamma_\mathrm{s}\,t}{2} - \eta_f\cos\phi_\mathrm{s}\,\sinh\frac{\Delta\Gamma_\mathrm{s}\,t}{2} \right. \qquad (5)$$
$$\left. +\eta_f\,q\,D\,\sin\phi_\mathrm{s}\,\sin\left(\Delta M_\mathrm{s}\,t\right)\right\},$$

where t is the proper time. The result of the flavor tagging (i.e. the determination of the initial b-meson flavor) is described by q, which takes the values of $q = +1$ if the signal meson is tagged as a $\mathrm{B_s}$ at production time, $q = -1$ if it is tagged as a $\overline{\mathrm{B}}_\mathrm{s}$, and $q = 0$ if the meson is untagged. The effect of the wrong-tag probability ω_tag is included in the dilution factor $D \equiv (1 - 2\omega_\mathrm{tag})$.

We see from (5) that untagged events give access to $\cos\phi_\mathrm{s}$ and $\Delta\Gamma_\mathrm{s}$. Given that the $\sin\phi_\mathrm{s}$ term and the tagging dilution D both modulate the ΔM_s oscillations, we need to introduce a control sample, e.g. $\mathrm{B_s} \to \mathrm{D_s}\pi$, to help in the determination of ΔM_s and of ω_tag.

1.3. $B_s \to J/\psi\phi$ Angular Analysis

The $\mathrm{B_s} \to \mathrm{J}/\psi\phi$ decay requires an angular analysis to separate the different CP eigenstates, which can be done using the linear polarization amplitudes $A_f(t)$. The transversity basis [6] enables to disentangle the CP components in terms of the so-called transversity angle θ. The one-angle angular differential distribution for $\mathrm{B_s} \to f$ is:

$$\frac{\mathrm{d}\,\Gamma[\mathrm{B_s}(t) \to f]}{\mathrm{d}\cos\theta} \propto (|A_0(t)|^2 + |A_\parallel(t)|^2)\,\frac{3}{8}\,(1+\cos^2\theta) + |A_\perp(t)|^2\,\frac{3}{4}\sin^2\theta\,. \quad (6)$$

The CP components are thus separated by their proper times and angular distributions. Finally, we introduce the observable fraction of CP-odd eigenstates at $t = 0$: $R_\mathrm{T} \equiv |A_\perp|^2 / \sum_{f=0,\parallel,\perp} |A_f|^2 \sim 20\%$.

1.4. $B_s \to D_s\pi$ Flavor-Specific Channel

ΔM_s can be extracted from the $\mathrm{B_s} \to \mathrm{D_s}\pi$ flavor-specific decay channel. Assuming no CP violation in the mixing, the decay rates are:

$$R\,(t, r) \propto \frac{e^{-\Gamma_\mathrm{s} t}}{2}\left\{\cosh\frac{\Delta\Gamma_\mathrm{s} t}{2} + r D \cos\left(\Delta M_\mathrm{s} t\right)\right\}, \quad (7)$$

where the results are $r = +1$ for a $\mathrm{B_s}$ candidate tagged as unmixed, $r = -1$ for a $\mathrm{B_s}$ tagged as mixed, and $r = 0$ for an untagged $\mathrm{B_s}$ candidate.

2. LHCb Full Monte Carlo Simulation

The LHCb experiment is designed to study rare b decays and CP violation. The high-precision measurements at LHCb will enable to test the CKM picture, and to probe physics beyond the Standard Model. The LHCb detector is a single-arm forward spectrometer, currently in its final construction phase. The main characteristics are the precise vertexing, and good tracking and particle identification.

We assume a $\mathrm{b\bar{b}}$ production cross-section of $\sigma_{\mathrm{b\bar{b}}} = 500\,\mu\mathrm{b}$ at the LHC. LHCb will run at a nominal luminosity of $\mathcal{L} = 2 \times 10^{32}\ \mathrm{cm^{-2}s^{-1}}$, corresponding to an annual (i.e. 10^7 s) integrated luminosity of $2\ \mathrm{fb^{-1}}$. The trigger system is designed to reduce the event rate to $\sim 2\,\mathrm{kHz}$.

The design and performance of the detector have been optimized using a realistic full Monte Carlo (MC) simulation. The pp collisions at $\sqrt{s} = 14\,\mathrm{TeV}$ are generated, including pileup. Particles are tracked through the detector setup, accounting for the detector's response, material, and spillover effects. After the trigger, the events are reconstructed off-line and signal events are identified by means of selection and flavor tagging algorithms.

The following is a summary of the ϕ_s studies described in [7].

2.1. Full Monte Carlo Results

The results from full MC studies are used to parameterize the fast simulation and assess the sensitivities to ϕ_s, using the following channels:

- $B_s \to J/\psi(\mu^+\mu^-)\phi(K^+K^-)$
- $B_s \to \eta_c(\pi^+\pi^-\pi^+\pi^-, \pi^+\pi^-K^+K^-, K^+K^-K^+K^-)\phi(K^+K^-)$
- $B_s \to J/\psi(\mu^+\mu^-)\eta(\gamma\gamma, \pi^+\pi^-\pi^0)$
- $B_s \to D_s^+(K^+K^-\pi^+)D_s^-(K^+K^-\pi^-)$

The $B_s \to D_s^-(K^+K^-\pi^-)\pi^+$ decay is used as control channel.

The results from the full simulation are summarized in Table 1. The yields correspond to the expected number of triggered and untagged off-line selected events with an integrated luminosity of $2\,fb^{-1}$. The background-to-signal ratio B/S is determined using mainly inclusive $b\bar{b}$ events. The mean of the per-event proper time errors is denoted by $< \tau_{fit}^{err} >$, and the proper time scale factor by Σ_τ (width of pull). Finally, ε_{tag} denotes the tagging efficiency and ω_{tag} the wrong tag fraction.

Table 1. Inputs from the full MC simulation used for the fast simulations.

Parameters	$J/\psi\phi$	$\eta_c\phi$	D_sD_s	$J/\psi\eta(\gamma\gamma)$	$J/\psi\eta(\pi\pi\pi)$	$D_s\pi$
$2\,fb^{-1}$ yield [k]	131	3	4	8.5	3	120
B/S	0.12	0.6	0.3	2.0	3.0	0.4
σ_{B_s} [MeV/c^2]	14	12	6	34	20	14
$< \tau_{fit}^{err} >$ [fs]	29.5	26.2	44.4	30.4	25.5	32.9
Σ_τ	1.22	1.16	1.26	1.22	1.32	1.21
ω_{tag} [%]	33	31	34	35	30	31
ε_{tag} [%]	57	66	57	63	62	63

The proper time and its error are extracted on an event-by-event basis using a least-squares fit. The distributions of the proper time errors τ_{fit}^{err} (scaled with Σ_τ) are shown in Fig. 3. Most channels have a proper time resolution below 40 fs, precise enough to resolve the fast B_s–$\overline{B}_s$ oscillations.

3. Sensitivity to the B_s–$\overline{B}_s$ Mixing Phase at LHCb

The sensitivities to the B_s–$\overline{B}_s$ mixing parameters are determined by means of fast parameterized simulations, with the results of Table 1 as

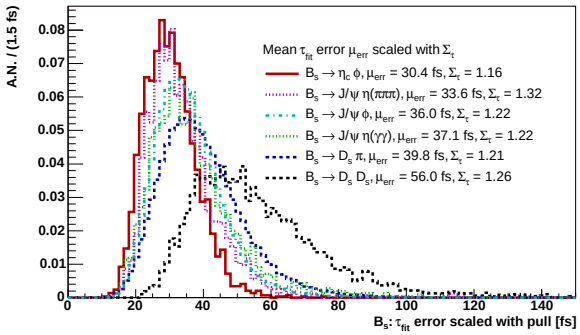

Fig. 3. Distribution of the proper time errors [fs] (scaled with Σ_τ) for the different B_s channels, as obtained from the full MC. The normalization is arbitrary.

inputs. We generate ~ 225 experiments with the nominal set of SM parameters $M_{B_s} = 5369.6\,\mathrm{MeV/c^2}$, $\Delta M_s = 17.5\,\mathrm{ps^{-1}}$, $\phi_s = -0.04$ rad, $\Delta\Gamma_s/\Gamma_s = 0.15$, $\tau_s = 1/\Gamma_s = 1.45$ ps, and $R_T = 0.2$ (for $B_s \to J/\psi\phi$).

3.1. Fast Monte Carlo

The different parameters are extracted by performing a likelihood fit to the mass, proper time, and transversity angle (for $B_s \to J/\psi\phi$) distributions, including a background contribution. The $\bar{b} \to \bar{c}c\bar{s}$ likelihood is simultaneously maximized with a similar likelihood for the $B_s \to D_s\pi$ control sample. We use the following models:

Mass: a Gaussian (signal) and an exponential (background) are used (see Fig. 4), which determine the signal and background probabilities.

Transversity angle: for the $B_s \to J/\psi\phi$ sample the distribution (6) is used, assuming a flat background (see Fig. 5).

Proper time: the signal decay rates are taken from (5) for the $\bar{b} \to \bar{c}c\bar{s}$ sample, from (7) for $B_s \to D_s\pi$, and exponentials are used for the background. The rates are weighted by an acceptance function. The signal proper time resolution function depends on $\tau_{\rm fit}^{\rm err}$ scaled with Σ_τ. We illustrate in Fig. 6 the rates for CP-even eigenstates, and in Fig. 7 the contributions to the proper time for the $B_s \to J/\psi\phi$ sample.

The background properties are determined from the B_s mass sidebands. The physics parameters, extracted in the signal region with all other parameters fixed, are ϕ_s, ΔM_s, $\Delta\Gamma_s/\Gamma_s$, $\tau_s = 1/\Gamma_s$, $\omega_{\rm tag}$, and R_T (for $B_s \to J/\psi\phi$). The sensitivity to a parameter corresponds to the rms of the distribution of the fit outputs.

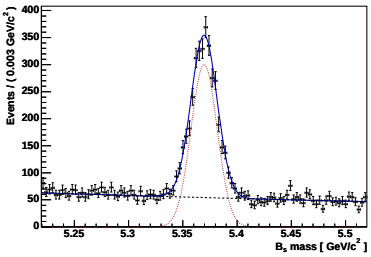

Fig. 4. Likelihood projection onto the mass [GeV/c^2] for $B_s \to \eta_c\phi$. Solid: all contributions. Dotted: signal. Dashed: background.

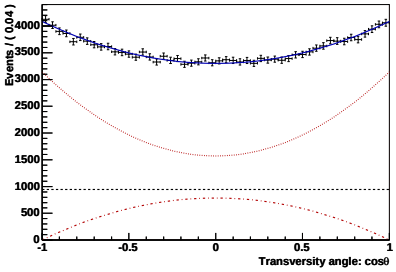

Fig. 5. Likelihood projection onto $\cos\theta$ for $B_s \to J/\psi\phi$ in the total mass window. Solid: all contributions. Dotted: CP-even. Dashed-dotted: CP-odd. Dashed: background.

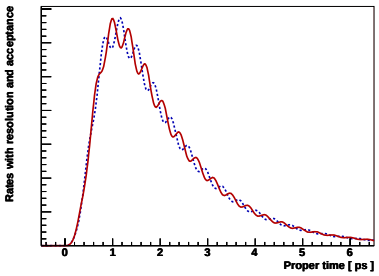

Fig. 6. Signal decay rates [ps] of $\bar{b} \to \bar{c}c\bar{s}$ transitions to CP-even eigenstates, with a 30% wrong-tag fraction, a 35 fs proper-time resolution, and $\phi_s = -0.2$ rad. Solid: tagged B_s. Dashed: tagged $\overline{B}_s$.

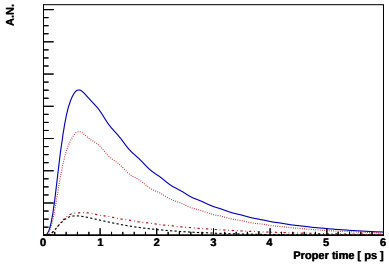

Fig. 7. Likelihood projection onto the proper time [ps] in the signal region, for $B_s \to J/\psi\phi$ events initially tagged as B_s. Solid: all contributions. Dotted: CP-even. Dashed-dotted: CP-odd. Dashed: background.

3.2. Fit Results

The sensitivities to ϕ_s from the simultaneous fits are given in Table 2. The best performance is from $B_s \to J/\psi\phi$, although we performed an angular analysis. The contribution from pure CP-eigenstates is small, but non-negligible. For $10\,\text{fb}^{-1}$, we get a statistical uncertainty $\sigma(\phi_s) = \pm 0.0098\,\text{rad}$.

The sensitivity to ϕ_s gently decreases with $|\phi_s|$, and does not depend much on ϕ_s. For instance, the significance is of $\sim 7\sigma$ for $\phi_s = -0.2$ rad from $B_s \to J/\psi\phi$ alone, with $2\,\text{fb}^{-1}$. In addition LHCb will have access

Table 2. Combined expected statistical errors on a SM ϕ_s with $2\,\text{fb}^{-1}$.

Channels	$\sigma(\phi_s)$ [rad]	Weight $(\sigma/\sigma_i)^2$ [%]
$B_s \to J/\psi\eta(\pi^+\pi^-\pi^0)$	0.142	2.3
$B_s \to D_sD_s$	0.133	2.6
$B_s \to J/\psi\eta(\gamma\gamma)$	0.109	3.9
$B_s \to \eta_c\phi$	0.108	3.9
Pure CP eigenstates	**0.060**	**12.7**
$B_s \to J/\psi\phi$	0.023	87.3
All CP eigenstates	**0.022**	**100.0**

to ΔM_s with a small statistical uncertainty $\sigma(\Delta M_s) = \pm 0.007\,\text{ps}^{-1}$ (from $B_s \to D_s\pi$, for $\Delta M_s = 17.5\,\text{ps}^{-1}$, and with $2\,\text{fb}^{-1}$).

4. Conclusions

We presented a method to extract the B_s–$\overline{B}_s$ mixing phase at LHCb, using $\bar{b} \to \bar{c}c\bar{s}$ quark-level transitions. The combined statistical sensitivity obtained is $\sigma(\phi_s) = \pm 0.022$ rad, corresponding to a $\sim 2\sigma$ measurement for a Standard Model $\phi_s = -0.04$ rad, and with $2\,\text{fb}^{-1}$. The sensitivity is dominated by $B_s \to J/\psi\phi$, with however a substantial $\sim 13\%$ contribution from decays to pure CP-eigenstates ($B_s \to \eta_c\phi$, $B_s \to D_sD_s$, $B_s \to J/\psi\eta$). It will allow LHCb to detect sizable New Physics effects.

In conclusion, LHCb has the potential to perform the first measurement of ϕ_s, to test the consistency with the Standard Model expectations, and to possibly uncover New Physics that may be hiding in the B_s–$\overline{B}_s$ mixing.

The author would like to thank Olivier Schneider for his careful reading of this writeup, and for his useful comments.

REFERENCES

[1] N. Cabibbo. *Phys. Rev. Lett.*, 10:531–533, 1963.
[2] M. Kobayashi and T. Maskawa. *Prog. Theor. Phys.*, 49:652–657, 1973.
[3] L. Wolfenstein. *Phys. Rev. Lett.*, 51:1945–1947, 1983.
[4] G.C. Branco, L. Lavoura, and J.P. Silva. *CP Violation*, Oxford U.P., 1999.
[5] I. Dunietz, R. Fleischer, and U. Nierste. *Phys. Rev.*, D63:114015, 2001.
[6] A.S. Dighe *et al. Phys. Lett.*, B369:144–150, 1996.
[7] L. Fernández. EPFL Ph. D. Thesis 3613, CERN-THESIS/2006-042, 2006.